Breaking the Hierarchy: Distributed Control & Economic Optimality in Microgrids

Florian Dörfler, John W. Simpson-Porco, and Francesco Bullo

***Abstract*—Modeled after the hierarchical control architecture of power transmission systems, a layering of primary, secondary, and tertiary control has become the standard operation paradigm for microgrids. Despite this superficial similarity, the control objectives in microgrids across these three layers are varied and ambitious, and they must be achieved while allowing for robust plug-and-play operation and maximal flexibility, without hierarchical decision making and time-scale separations. In this work, we explore control strategies for these three layers and illuminate some possibly-unexpected connections and dependencies among them. Building from a first-principle analysis of decentralized primary droop control, we study centralized, decentralized, and distributed architectures for secondary frequency regulation. We find that averaging-based distributed controllers using communication among the generation units offer the best combination of flexibility and performance. We further leverage these results to study constrained AC economic dispatch in a tertiary control layer. Surprisingly, we show that the minimizers of the economic dispatch problem are in one-to-one correspondence with the set of steady-states reachable by droop control. In other words, the adoption of droop control is necessary and sufficient to achieve economic optimization. This equivalence results in simple guidelines to select the droop coefficients, which include the known criteria for power sharing. We illustrate the performance and robustness of our designs through simulations.**

I. Introduction

With the goal of integrating distributed renewable generation and energy storage systems, the concept of a *microgrid* has recently gained popularity [2]–[5]. Microgrids are low-voltage electrical distribution networks, heterogeneously composed of distributed generation, storage, load, and managed autonomously from the larger transmission network. Microgrids are able to connect to a larger electric power system, but are also able to island themselves and operate independently.

Distributed energy sources in a microgrid generate either DC or variable frequency AC power, and are interfaced with an AC grid via power electronic DC/AC *inverters*. Through these inverters, cooperative actions must be taken to ensure synchronization, voltage stability, power balance, load sharing, and economic operation [6], [7]. A variety of control and decision architectures — ranging from centralized to fully decentralized — have been proposed to address these challenges [5]–[8]. In transmission networks, the different control tasks are separated in their time scales and aggregated into a hierarchy. Similar operation layers have been proposed for microgrids.

This work was supported in part by UCLA startup funds, the National Science and Engineering Research Council of Canada, and the National Science Foundation NSF CNS-1135819. A preliminary version of part of the results in this document has been presented in [1].

F. Dörfler is with the Department of Electrical Engineering, University of California Los Angeles. Email: dorfler@seas.ucla.edu. J. W. Simpson-Porco and F. Bullo are with the Mechanical Engineering Department, University of California Santa Barbara. Email: {johnwsimpsonporco,bullo}@engineering.ucsb.edu.

Control Hierarchy in Transmission Systems: The foundation of this hierarchy, termed *primary control*, must rapidly balance generation and demand, while sharing the load, synchronizing the AC voltage frequencies, and stabilizing their magnitudes. This is accomplished via decentralized *droop* control, where generators are controlled such that their power injections are proportional to their voltage frequencies and magnitudes [9].

Droop controllers induce steady-state errors in frequency and voltage magnitudes, which are corrected in a *secondary control* layer. At the transmission level, the network is partitioned into control areas, and a few selected generators then balance local generation in each area with load and inter-area power transfers. Termed *automatic generation control* (AGC), this architecture is based on centralized integral control and operates on a slower time scale than primary control [10].

The operating point stabilized by primary/secondary control is scheduled in a *tertiary* control layer, to establish fair load sharing among the sources, or to dispatch the generation to minimize operational costs. In conventional operation of bulk power systems, an economic dispatch is optimized offline, in a centralized fashion, using precise load forecasts [11]. In [12]–[15] it has been shown that the dynamics of a power transmission system with synchronous generators and AGC naturally optimize variations of the economic dispatch.

Adaption of Control Layers to Microgrids: With regards to primary control in microgrids, inverters are typically controlled to emulate the droop characteristic of synchronous generators [3]–[7]. Despite forming the foundation for the operation of microgrids, networks of droop-controlled inverters have only recently been subject to a rigorous analysis. In [16], [17], the authors presented necessary and sufficient stability conditions in a droop-controlled microgrid. We also refer to [18]–[23] for alternative analyses resulting in sufficient conditions.

Secondary control strategies akin to AGC have been adapted to microgrids. In [12], decentralized and centralized integral controllers are studied. In [24] (respectively [25]) distributed integral controllers based on all-to-all frequency (respectively power output) averaging are proposed. In [26], the trade-off between time-scale separation and achievable decentralized performance is analyzed. In [27] discrete-time averaging-based approaches are proposed for secondary regulation and tertiary-level economic dispatch. In [28], a decentralized state feedback is designed. All of these decentralized and distributed secondary control strategies share the common disadvantage that the primary and secondary control loops may interact in an adverse way unless a time-scale separation is enforced or the control gains are carefully tuned. In [16], the authors proposed a distributed averaging-based integral control strategy that does not require any tuning or a time-scale separation.

Transmission Level vs. Distribution & Microgrids: While the hierarchical architecture has been adapted from the transmission level to microgrids, the control challenges and architecture limitations imposed by the microgrid framework are as diverse as they are daunting. The low levels of inertia in microgrids mean that primary control must be fast and reliable to maintain voltages, frequencies, and power flows within acceptable tolerances, while the highly variable and distributed nature of microgrids preclude centralized control strategies of any kind. Microgrid controllers must be able to adapt in real time to unknown and variable loads and network conditions. In short, the three layers of the control hierarchy for microgrids must allow for as close to plug-and-play operation as possible, be either distributed or completely decentralized, and operate seamlessly without a pre-imposed separation of time scales.

Contributions and Contents: In this article, we present a comprehensive modeling framework for microgrids with heterogenous components and different control tasks; see Section II. Building on our previous work [16], we study the decentralized limitations of primary control in Section III. In particular, we show that the set of feasible setpoints for power flow dispatch is in one-to-one correspondence with the set of steady-states reachable via decentralized droop control.

In Section IV, we study several decentralized and distributed secondary integral control strategies. We first discuss the limitations of decentralized secondary integral control akin to AGC. Next, we study distributed secondary control strategies. We provide a rigorous analysis for the strategies proposed in [24], [25] for a proper choice of control gains and compare them to our earlier work [16] with regards to tuning limitations and communication complexity. We show that all these distributed strategies successfully regulate the frequency, maintain the injections and stability properties of the primary droop controller, and do not require any separation of time scales. Finally, we demonstrate that these properties are maintained when only a subset of generating units participate in secondary control action. The effectiveness of these distributed secondary control strategies has been confirmed in experiments [24], [29].

In Section V, we study tertiary control policies that minimize an economic dispatch problem. We leverage a recently discovered relation between AC and DC power flows [30], [31] and show that the set of minimizers of the nonlinear and non-convex AC economic dispatch optimization problem are in one-to-one correspondence with the minimizers of a convex DC dispatch problem. Our next result shows a surprising symbiotic relationship between primary/secondary control and tertiary. We show that the minimum of the AC economic dispatch can be achieved by a decentralized droop control design. Conversely, every droop controller results in a steady-state which is the minimizer of some AC economic dispatch. We deduce, among others, that the optimal droop coefficients are inversely proportional to the marginal cost of generation.

In Section VI, we illustrate the performance and robustness of our controllers with a simulation study of the IEEE 37 bus distribution network. Finally, Section VII concludes the paper. The remainder of this section introduces some preliminaries.

Preliminaries and Notation

Vectors and matrices: Given a finite set $\mathcal{V}$, let $|\mathcal{V}|$ denote its cardinality. Given a finite index set $\mathcal{I}$ and a real-valued one-dimensional array $\{x_1, \dots, x_{|\mathcal{I}|}\}$, the associated vector and diagonal matrix are $x \in \mathbb{R}^{|\mathcal{I}|}$ and $\mathrm{diag}(\{x_i\}_{i\in\mathcal{I}}) \in \mathbb{R}^{|\mathcal{I}|\times|\mathcal{I}|}$. Let $\mathbf{1}_n$ and $\mathbf{0}_n$ be the n-dimensional vectors of unit and zero entries. We denote the diagonal vector space $\mathrm{Span}\,(\mathbf{1}_n)$ by $\mathbb{1}_n$ and its orthogonal complement by $\mathbb{1}_n^{\perp} \triangleq \{x \in \mathbb{R}^n : \mathbf{1}_n^T x = 0\}$.

Algebraic graph theory: We denote by $G(\mathcal{V}, \mathcal{E}, A)$ an undirected and weighted graph, where $\mathcal{V}$ is node set, $\mathcal{E} \subseteq \mathcal{V}\times\mathcal{V}$ is the edge set, and $A = A^T \in \mathbb{R}^{|\mathcal{V}|\times|\mathcal{V}|}$ is the *adjacency matrix*. If a number $\ell \in \{1, \dots, |\mathcal{E}|\}$ and an arbitrary direction are assigned to each edge, the *incidence matrix* $B \in \mathbb{R}^{|\mathcal{V}|\times|\mathcal{E}|}$ is defined component-wise as $B_{k\ell} = 1$ if node k is the sink node of edge ℓ and as $B_{k\ell} = -1$ if node k is the source node of edge ℓ; all other elements are zero. The *Laplacian matrix* is $L \triangleq B\mathrm{diag}(\{a_{ij}\}_{\{i,j\}\in\mathcal{E}})B^T$. If the graph is connected, then $\ker(B^T) = \ker(L) = \mathbb{1}_{|\mathcal{V}|}$. For acyclic graphs, $\ker(B) = \emptyset$, and for every $x \in \mathbb{1}_{|\mathcal{V}|}^{\perp}$ there is a unique $\xi \in \mathbb{R}^{|\mathcal{E}|}$ satisfying *Kirchoff's Current Law* (KCL) $x = B\xi$. In a circuit, x are the nodal injections, and ξ are the associated edge flows.

Geometry on the n-torus: The set $\mathbb{S}^1$ denotes the *circle*, an *angle* is a point $\theta \in \mathbb{S}^1$, and an *arc* is a connected subset of $\mathbb{S}^1$. Let $|\theta_1 - \theta_2|$ be the *geodesic distance* between two angles $\theta_1, \theta_2 \in \mathbb{S}^1$. The *$n$-torus* is $\mathbb{T}^n = \mathbb{S}^1 \times \cdots \times \mathbb{S}^1$. For $\gamma \in [0, \pi/2[$ and a graph $G(\mathcal{V}, \mathcal{E}, \cdot)$, let $\overline{\Delta}_G(\gamma) = \{\theta \in \mathbb{T}^{|\mathcal{V}|} : \max_{\{i,j\}\in\mathcal{E}} |\theta_i - \theta_j| \leq \gamma\}$ be the closed set of angle arrays $\theta = (\theta_1, \dots, \theta_n)$ with neighboring angles θ_i and θ_j, $\{i, j\} \in \mathcal{E}$ no further than γ apart. Let $\Delta_G(\gamma)$ be the interior of $\overline{\Delta}_G(\gamma)$.

II. MICROGRIDS AND THEIR CONTROL CHALLENGES

A. Microgrids and AC Circuits

In this paper, we adopt the standard model of a microgrid as synchronous linear circuit with admittance matrix $Y \in \mathbb{C}^{n\times n}$. The associated connected, undirected, and complex-weighted graph is $G(\mathcal{V}, \mathcal{E}, A)$ with node set (or buses) $\mathcal{V} = \{1, \dots, n\}$, edge set (or branches) $\mathcal{E} \subset \mathcal{V} \times \mathcal{V}$, and symmetric weights (or admittances) $a_{ij} = -Y_{ij} = -Y_{ji} \in \mathbb{C}$ for each branch $\{i, j\} \in \mathcal{E}$. We restrict ourselves to *acyclic* (also called radial) topologies prevalent in low-voltage distribution networks.

To each node $i \in \mathcal{V}$, we associate an electrical power injection $S_{\mathrm{e},i} = P_{\mathrm{e},i} + \sqrt{-1}Q_{\mathrm{e},i} \in \mathbb{C}$ and a voltage phasor $V_i = E_i e^{\sqrt{-1}\theta_i} \in \mathbb{C}$ corresponding to the magnitude $E_i > 0$ and the phase angle $\theta_i \in \mathbb{S}^1$ of a harmonic voltage solution to the AC circuit equations. The complex vector of nodal power injections is then $S_{\mathrm{e}} = V \circ (YV)^C$, where ^{C} denotes the complex conjugation $\circ$ is the Hadamard (element-wise) product. For *inductive lines*, the admittance matrix $Y \in \mathbb{C}^{n\times n}$ is purely imaginary, and the active/reactive nodal power injections are

$$P_{\mathrm{e},i} = \sum\nolimits_{j=1}^{n} \Im\mathfrak{m}(Y_{ij}) E_i E_j \sin(\theta_i - \theta_j)\,, \qquad i \in \mathcal{V}\,, \quad (1a)$$

$$Q_{\mathrm{e},i} = -\sum\nolimits_{j=1}^{n} \Im\mathfrak{m}(Y_{ij}) E_i E_j \cos(\theta_i - \theta_j)\,, \quad i \in \mathcal{V}. \quad (1b)$$

We adopt the standard *decoupling approximation* [4], [9] where all voltage magnitudes E_i are constant in the active power injections (1a) and $P_{\mathrm{e},i} = P_{\mathrm{e},i}(\theta)$. By continuity and exponential stability, our results are robust to bounded voltage dynamics [16], [30], which we illustrate via simulations.

We partition the set of buses into loads and inverters, $\mathcal{V} = \mathcal{V}_L \cup \mathcal{V}_I$, and denote their cardinalities by $n \triangleq |\mathcal{V}|$, $n_L \triangleq |\mathcal{V}_L|$, and $n_I \triangleq |\mathcal{V}_I|$. Each load $i \in \mathcal{V}_L$ demands a constant amount of active power $P_i^* \in \mathbb{R}$ and satisfies the power flow equation

$$0 = P_i^* - P_{\mathrm{e},i}(\theta)\,, \quad i \in \mathcal{V}_L\,. \tag{2}$$

We refer to the buses $\mathcal{V}_L$ strictly as *loads*, with the understanding that they can be either loads or constant-power sources.

We denote the rating (maximal power injection) of inverter $i \in \mathcal{V}_I$ by $\overline{P}_i \geq 0$. As a necessary feasibility condition, we assume throughout this article that the total load $\sum_{i\in\mathcal{V}_L} P_i^*$ is a net demand serviceable by the inverters' maximal generation:

$$0 \leq -\sum\nolimits_{i\in\mathcal{V}_L} P_i^* \leq \sum\nolimits_{i\in\mathcal{V}_I} \overline{P}_i\,. \tag{3}$$

After appropriate inner control loops are established, an inverter behaves much like a *controllable voltage source* behind a reactance [4], which is the standard model in the literature.

B. Primary Droop Control

The *frequency droop controller* is the main technique for primary control in microgrids [3]–[7]. At inverter i, the frequency $\dot\theta_i$ is controlled to be proportional to the measured (see [4] for details) power injection $P_{\mathrm{e},i}(\theta)$ according to

$$D_i\dot\theta_i = P_i^* - P_{\mathrm{e},i}(\theta)\,, \quad i \in \mathcal{V}_I\,, \tag{4}$$

where $P_i^* \in [0, \overline{P}_i]$ is a *nominal injection setpoint*, and the proportionality constant $D_i \geq 0$ is referred to as the (inverse) *droop coefficient*. In this notation, $\dot\theta_i$ is actually the frequency error $\omega_i - \omega^*$, where ω^* is the nominal network frequency.

The droop-controlled microgrid is then described by the nonlinear, differential-algebraic equations (DAE) (2),(4).

Remark 1: **(Droop Controllers for Non-Inductive Networks).** The equations (1)-(4) are valid for purely inductive lines without resistive losses. This assumption is typically justified, as the inverter output impedances can be controlled to dominate over the network impedances [32]. Nonetheless, our analysis can be easily extended towards more general networks, including resistive/capacitive lines [4, Chapter 19.4], constant R/X ratio lines [33, Eq. (7)-(10)], and (by continuity) networks with sufficiently uniform R/X ratio lines. □

C. Secondary Frequency Control

The droop controller (4) induces a static error in the steady-state frequency. If the droop-controlled system (2), (4) settles to a frequency-synchronized solution, $\dot\theta_i(t) = \omega_{\mathrm{sync}} \in \mathbb{R}$ for all $i \in \mathcal{V}$, then summing over all equations (2),(4) yields the synchronous frequency ω_{sync} as the *scaled power imbalance*

$$\omega_{\mathrm{sync}} \triangleq \frac{\sum_{i\in\mathcal{V}} P_i^*}{\sum_{i\in\mathcal{V}_I} D_i}\,. \tag{5}$$

Notice that ω_{sync} is zero if and only if the nominal injections P_i^* are balanced: $\sum_{i\in\mathcal{V}} P_i^* = 0$. Since the loads are generally unknown and variable, it is not possible to select the nominal source injections to balance them. Likewise, to render ω_{sync} small, the coefficients D_i cannot be chosen arbitrary large, since the primary control becomes slow and possibly unstable.

To eliminate this static error in network frequency, additional *secondary control* inputs $u_i : \mathbb{R}_{\geq 0} \to \mathbb{R}$ are needed. The controlled inverter equation (4) then becomes

$$D_i\dot\theta_i = P_i^* - P_{\mathrm{e},i}(\theta) + u_i(t)\,. \tag{6}$$

If there is a synchronized solution to the secondary-controlled equations (2),(6) with frequency ω^*_{sync} and steady-state secondary control inputs $u_i^* = \lim_{t\to\infty} u_i(t)$, then we obtain it as

$$\omega^*_{\mathrm{sync}} = \frac{\sum_{i\in\mathcal{V}} P_i^* + \sum_{j\in\mathcal{V}_I} u_i^*}{\sum_{i\in\mathcal{V}_I} D_i} = \omega_{\mathrm{sync}} + \frac{\sum_{j\in\mathcal{V}_I} u_i^*}{\sum_{i\in\mathcal{V}_I} D_i}\,. \tag{7}$$

Clearly, there are many choices for the inputs u_i^* to achieve the control objective $\omega^*_{\mathrm{sync}} = 0$. However, the inputs u_i^* are typically constrained due to additional performance criteria.

D. Tertiary Operational Control

A tertiary operation and control layer has the objective to minimize an *economic dispatch problem*, that is, an appropriate quadratic cost of the accumulated generation:

$$\begin{aligned}
&\underset{\theta\in\mathbb{T}^n,\, u\in\mathbb{R}^{n_I}}{\text{minimize}} && f(u) = \sum\nolimits_{i\in\mathcal{V}_I} \frac{1}{2}\alpha_i u_i^2 && && \text{(8a)}\\
&\text{subject to} && P_i^* + u_i = P_{\mathrm{e},i}(\theta) && \forall\, i \in \mathcal{V}_I\,, && \text{(8b)}\\
& && P_i^* = P_{\mathrm{e},i}(\theta) && \forall\, i \in \mathcal{V}_L\,, && \text{(8c)}\\
& && |\theta_i - \theta_j| \leq \gamma_{ij}^{(\mathrm{AC})} && \forall\, \{i,j\} \in \mathcal{E}\,, && \text{(8d)}\\
& && P_{\mathrm{e},i}(\theta) \in [0, \overline{P}_i] && \forall\, i \in \mathcal{V}_I\,, && \text{(8e)}
\end{aligned}$$

Here, $\alpha_i > 0$ is the marginal cost for source $i \in \mathcal{V}_I$. The decision variables are the angles θ and secondary control inputs u. The non-convex equality constraints (8b)-(8c) are the nonlinear steady-state secondary control equations (8b)-(8c), the *security constraint* (8d) limits the power flow on each branch $\{i,j\} \in \mathcal{E}$ with $\gamma_{ij}^{(\mathrm{AC})} \in [0, \pi/2[$, and (8e) is a *generation constraint*.

Two typical instances of the economic dispatch (8) are as follows: For $P_i^* = 0$, u_i equals $P_{\mathrm{e},i}(\theta)$, and the total generation cost is penalized. If the nominal generation setpoints P_i^* are positive (e.g., scheduled according to some load forecast), then u_i^* is the operating reserve to meet the real-time demand.

E. Heterogeneous Microgrids with Additional Components

In the following, we briefly list additional components in a microgrid, which can be captured by the model (1a),(2),(4).

Synchronous machines: Synchronous generators (respectively motors) are sources (respectively loads) with dynamics

$$M_i\ddot\theta_i + D_i\dot\theta_i = P_i^* - P_{\mathrm{e},i}(\theta)\,, \tag{9}$$

where $M_i > 0$ is the inertia term, and the damping coefficient $D_i = D_{\mathrm{diss},i} + D_{\mathrm{droop},i} > 0$ combines dissipation $D_{\mathrm{diss},i}\dot\theta_i$ and a droop term $D_{\mathrm{droop},i}\dot\theta_i$ [9]. The constant power injection $P_i^* \in \mathbb{R}$ is positive for a generator and negative for a load. As shown in [34, Theorem 5.1], the synchronous machine model (9) is topologically equivalent to a first-order model of the form (4).

Inverters with measurement delays: The delay between the power measurement $P_{\mathrm{e},i}(\theta)$ at an inverter $i \in \mathcal{V}_I$ and the droop control actuation (4) can be explicitly modeled by a first-order lag filter with state $s_i \in \mathbb{R}$ and time constant $T_i > 0$:

$$\begin{aligned}
D_i\dot\theta_i &= P_i^* - s_i\,,\\
T_i\dot s_i &= P_{\mathrm{e},i}(\theta) - s_i\,.
\end{aligned} \tag{10}$$

As shown in [23, Lemma 4.1], after a linear change of variables, the dynamics (10) equal the machine dynamics (9).

Frequency-dependent loads: If the demand depends on the frequency [13]–[16], [20], [26], that is, the left-hand side of (2) is $D_i\dot{\theta}_i$ with $D_i > 0$, the load dynamics (2) are identical to inverter dynamics (4) with $P_i^* \leq 0$. In this case, the microgrid is modeled by ordinary differential equations. This frequency-dependence does not alter the local stability of equilibria [30].

In summary, all results pertaining to equilibria of the microgrid model (2),(4) and their local stability extend to synchronous machines, inverters with measurement delays, and frequency-dependent loads. Likewise, all secondary or tertiary control strategies can be equally applied. With these extensions in mind, we focus on the microgrid model (2),(4).

III. Decentralized Primary Control Strategies

In this section, we study the fundamental properties of the droop-controlled microgrid (2),(4). In Section IV, we design appropriate secondary controllers, which preserve the properties of primary control even if the load profile is unknown.

A. Symmetries, Synchronization, and Transformations

The microgrid equations (2),(4) feature an inherent *rotational symmetry*: they are invariant under a rigid rotation of all angles. Formally, let $\mathrm{rot}_s(r) \in \mathbb{S}^1$ be the rotation of a point $r \in \mathbb{S}^1$ counterclockwise by the angle $s \in [0, 2\pi]$. For $(r_1, \dots, r_n) \in \mathbb{T}^n$, define the equivalence class

$$[(r_1, \dots, r_n)] = \{(\mathrm{rot}_s(r_1), \dots, \mathrm{rot}_s(r_n)) \in \mathbb{T}^n : s \in [0, 2\pi]\}\,.$$

Thus, a synchronized solution $\theta^*(t)$ of (2),(4) is part of a one-dimensional connected *synchronization manifold* $[\theta^*]$. For $\omega_{\text{sync}} = 0$, a synchronization manifold is also an equilibrium manifold of (2),(4). In the following, when we refer to a synchronized solution as "stable" or "unique", these properties are to be understood modulo rotational symmetry.

We make use of this rotational symmetry and establish the equivalence of three different problems: stability of synchronized solutions for primary control, stability of equilibria with appropriate constant secondary control inputs u_i, and stability of equilibria for a new system in a set of shifted coordinates.

Recall that, without secondary control, the synchronous frequency ω_{sync} is the scaled power imbalance (5). By transforming to a rotating coordinate frame with frequency ω_{sync}, that is, $\theta_i(t) \mapsto \mathrm{rot}_{\omega_{\text{sync}} t}(\theta_i(t))$ (with slight abuse of notation, we maintain the variable θ), a synchronized solution of (2),(4) is equivalent to an equilibrium of the *shifted control system*

$$0 = \widetilde{P}_i - P_{\mathrm{e},i}(\theta)\,, \qquad i \in \mathcal{V}_L\,, \tag{11a}$$

$$D_i\dot{\theta}_i = \widetilde{P}_i - P_{\mathrm{e},i}(\theta)\,, \qquad i \in \mathcal{V}_I\,, \tag{11b}$$

where the *shifted power injections* are $\widetilde{P}_i = P_i^*$ for $i \in \mathcal{V}_L$, and $\widetilde{P}_i = P_i^* - D_i\omega_{\text{sync}}$ for $i \in \mathcal{V}_I$. We emphasize that the shifted injections in (11) are balanced: $\widetilde{P} \in \mathbb{1}_n^{\perp}$. Notice that, equivalently to transforming to a rotating frame with frequency ω_{sync} (or replacing P by $\widetilde{P}$), we can assume that the secondary control input in (2),(6) takes the constant value $u_i = -D_i\omega_{\text{sync}}$ for all $i \in \mathcal{V}_I$ to arrive at the shifted control system (11).

We summarize these observations in the following lemma.

Lemma 3.1: **(Synchronization Equivalences).** The following statements are equivalent:

(i) The primary droop-controlled microgrid (2),(4) possesses a locally exponentially stable and unique synchronization manifold $t \mapsto [\theta(t)] \subset \mathbb{T}^n$ for all $t \geq 0$;

(ii) The secondary droop-controlled microgrid (2),(6) with constant secondary-control input $u_i = -D_i\omega_{\text{sync}}$ for all $i \in \mathcal{V}_I$ possesses a locally exponentially stable and unique equilibrium manifold $[\bar{\theta}] \subset \mathbb{T}^n$;

(iii) The shifted control system (11) possesses a locally exponentially stable and unique equilibrium $[\tilde{\theta}] \subset \mathbb{T}^n$.

If the equivalent statements (i)-(iii) are true, then all systems have the same synchronization manifolds $[\theta(t)] = [\bar{\theta}] = [\tilde{\theta}] \subset \mathbb{T}^n$ and the same power injections $P_{\mathrm{e}}(\theta(t)) = P_{\mathrm{e}}(\bar{\theta}) = P_{\mathrm{e}}(\tilde{\theta})$. Additionally, $\theta(t) = \mathrm{rot}_{\omega_{\text{sync}} t}(\xi_0)$ for some $\xi_0 \in [\bar{\theta}] = [\tilde{\theta}]$.

In light of Lemma 3.1, we restrict the discussion in this section to the shifted control system (11).

Observe also that equilibria of (11) are invariant under *constant scaling* of all droop coefficients: if D_i is replaced by $D_i \cdot \beta$ for some $\beta \in \mathbb{R}$, then ω_{sync} changes to $\omega_{\text{sync}}/\beta$. Since the product $D_i \cdot \omega_{\text{sync}}$ remains constant, the equilibria of (11) do not change. Moreover, if $\beta > 0$, then the stability properties of equilibria do not change since time can be rescaled as $t \mapsto t \cdot \beta$.

B. Existence, Uniqueness, & Stability of Synchronization

In vector form, the equilibria of (11) satisfy

$$\widetilde{P} = B\mathcal{A}\,\mathbf{sin}(B^T\theta)\,, \tag{12}$$

where $B \in \mathbb{R}^{|\mathcal{V}|\times|\mathcal{E}|}$ is the incidence matrix of the network and $\mathcal{A} = \mathrm{diag}(\{\mathfrak{Im}(Y_{ij})E_iE_j\}_{\{i,j\}\in\mathcal{E}})$ is the diagonal matrix of line susceptances, weighted by voltage magnitudes. For an acyclic network, $\ker(B) = \emptyset$, and the unique vector of branch power flows $\xi \in \mathbb{R}^{|\mathcal{E}|}$ (associated to the shifted power injections $\widetilde{P}$) is given by the KCL as $\xi = B^\dagger\widetilde{P} = (B^TB)^{-1}B^T\widetilde{P}$.

Hence, the equilibrium equations (12) equivalently read as

$$\xi = \mathcal{A}\,\mathbf{sin}(B^T\theta)\,. \tag{13}$$

Due to boundedness of the sinusoid, a necessary condition for solvability of equation (13) is $\|\mathcal{A}^{-1}\xi\|_\infty < 1$. The following result shows that this condition is also sufficient and guarantees stability of an equilibrium manifold of (11) [16, Theorem 2].

Theorem 3.2: **(Existence and Stability of Synchronization).** Consider the shifted control system (11). Let $\xi \in \mathbb{R}^{|\mathcal{E}|}$ be the unique vector of power flows satisfying the KCL, given by $\xi = B^\dagger\widetilde{P}$. The following two statements are equivalent:

(i) ***Synchronization:*** there exists an arc length $\gamma \in [0, \pi/2[$ such that the shifted control system (11) possesses a locally exponentially stable and unique equilibrium manifold $[\theta^*] \subset \overline{\Delta}_G(\gamma)$;

(ii) ***Flow feasibility:*** the power flow is feasible, that is,

$$\Gamma \triangleq \|\mathcal{A}^{-1}\xi\|_\infty < 1. \tag{14}$$

If the equivalent statements (i) and (ii) hold true, then the quantities $\Gamma \in [0, 1[$ and $\gamma \in [0, \pi/2[$ are related uniquely via $\Gamma = \sin(\gamma)$, and $\mathbf{sin}(B^T\theta^*) = \mathcal{A}^{-1}\xi$.

While Theorem 3.2 gives the necessary and sufficient condition for the existence of a synchronized solution, it offers no guidance on how to select the droop control parameters (P_i^*, D_i) to satisfy the actuation constraint $P_{\mathrm{e},i}(\theta) \in [0, \overline{P}_i]$, or to achieve a set of desired steady-state power injections. We will address these questions in the following subsections.

C. Power Flow Constraints and Proportional Power Sharing

One desired objective in a microgrid is that all sources share the load in a fair way according to their power ratings [4]–[6]:

Definition 1: **(Proportional Power Sharing).** Consider an equilibrium manifold $[\theta^*] \subset \mathbb{T}^n$ of the shifted control system (11). The inverters $\mathcal{V}_I$ share the total load $\sum_{i\in\mathcal{V}_L} P_i^*$ *proportionally according to their power ratings* if for all $i, j \in \mathcal{V}_I$

$$P_{e,i}(\theta^*)/\overline{P}_i = P_{e,j}(\theta^*)/\overline{P}_j \,. \tag{15}$$

We also define a useful choice of droop coefficients.

Definition 2: **(Proportional Droop Coefficients and Nominal Injection Setpoints).** The droop coefficients and injections setpoints are selected proportionally if for all $i, j \in \mathcal{V}_I$

$$P_i^*/D_i = P_j^*/D_j \;\text{ and }\; P_i^*/\overline{P}_i = P_j^*/\overline{P}_j \,. \tag{16}$$

A proportional choice of droop control coefficients leads to a fair load sharing among the inverters according to their ratings and subject to their actuation constraints [16, Theorem 7]:

Theorem 3.3: **(Power Flow Constraints and Power Sharing).** Consider an equilibrium manifold $[\theta^*] \subset \mathbb{T}^n$ of the shifted control system (11). Let the droop coefficients be selected proportionally. The following statements are equivalent:

(i) ***Injection constraints:*** $0 \leq P_{e,i}(\theta^*) \leq \overline{P}_i, \quad \forall i \in \mathcal{V}_I$;

(ii) ***Serviceable load:*** $0 \leq -\sum_{i\in\mathcal{V}_L} P_i^* \leq \sum_{j\in\mathcal{V}_I} \overline{P}_j$.

Moreover, the inverters share the total load $\sum_{i\in\mathcal{V}_L} P_i^*$ proportionally according to their power ratings.

Theorem 3.3 also holds for lossy and meshed circuits [16].

D. Power Flow Shaping

We now address the following "controllability" question: given a set of desired power injections for the inverters, can one select the droop coefficients to generate these injections?

We define a *power injection setpoint* as a point of power balance, at fixed load demands and subject to the basic feasibility condition given in Theorem 3.2.

Definition 3: **(Feasible Power Injection Setpoint).** Let $\gamma \in [0, \pi/2[$. A vector $P^{\text{set}} \in \mathbb{R}^n$ is a *γ-feasible power injection setpoint* if it satisfies the following three properties:

(i) ***Power balance:*** $P^{\text{set}} \in \mathbb{1}_n^\perp$;

(ii) ***Load invariance:*** $P_i^{\text{set}} = P_i^*$ for all loads $i \in \mathcal{V}_L$;

(iii) ***γ-feasibility:*** the associated branch power flows $\xi^{\text{set}} = B^\dagger P^{\text{set}}$ are feasible, that is, $\|\mathcal{A}^{-1}\xi^{\text{set}}\|_\infty \leq \sin(\gamma)$.

The next result characterizes the relationship between droop controller designs and γ-feasible injection setpoints. For simplicity, we omit the singular case where $\omega_{\text{sync}} = 0$, since in this case the droop coefficients offer no control over the steady-state inverter injections $P_{e,i}(\theta^*) = P_i^* - D_i\omega_{\text{sync}}$.

Theorem 3.4: **(Power Flow Shaping).** Consider the shifted control system (11). Assume $\omega_{\text{sync}} \neq 0$, let $P^{\text{set}} \in \mathbb{1}_n^\perp$, and let $\gamma \in [0, \pi/2[$. The following statements are equivalent:

(i) ***Coefficient selection:*** there exists a selection of droop coefficients D_i, $i \in \mathcal{V}_I$, such that the steady-state injections satisfy $P_e(\theta^*) = P^{\text{set}}$, with $[\theta^*] \subset \overline{\Delta}_G(\gamma)$;

(ii) ***Feasibility:*** P^{set} is a γ-feasible power injection setpoint.

If the equivalent statements (i) and (ii) hold true, then the quantities D_i and P_i^{set} are related with arbitrary $\beta \neq 0$ as

$$D_i = \beta(P_i^* - P_i^{\text{set}}) \,, \quad i \in \mathcal{V}_I \,. \tag{17}$$

Moreover, $[\theta^*]$ is locally exponentially stable if and only if $\beta(P_i^* - P_i^{\text{set}})$ is nonnegative for all $i \in \mathcal{V}_I$.

Proof: **(i) $\Longrightarrow$ (ii):** Since $\theta^* \in \overline{\Delta}_G(\gamma)$ and $P_e(\theta^*) \in \mathbb{1}_n^\perp$, Theorem 3.2 shows that P^{set} is a γ-feasible injection setpoint.

(ii) $\Longrightarrow$ (i): Let P^{set} be a γ-feasible injection setpoint. Consider the droop coefficients $D_i = \beta(P_i^* - P_i^{\text{set}})$. Since $\omega_{\text{sync}} \neq 0$, for each $i \in \mathcal{V}_I$ we obtain the steady-state injection

$$\begin{aligned} P_{e,i}(\theta^*) &= \widetilde{P}_i = P_i^* - D_i\omega_{\text{sync}} \\ &= P_i^* - \beta(P_i^* - P_i^{\text{set}})\frac{1}{\beta}\underbrace{\frac{\sum_{i\in\mathcal{V}} P_i^*}{\sum_{i\in\mathcal{V}_I}(P_i^* - P_i^{\text{set}})}}_{=1} = P_i^{\text{set}} \,, \end{aligned}$$

where we used $\sum_{i\in\mathcal{V}_I} P_i^{\text{set}} = -\sum_{i\in\mathcal{V}_L} P_i^*$. Since $P_{e,i}(\theta^*) = P_i^* = P_i^{\text{set}}$ for each $i \in \mathcal{V}_L$, we have $P_e(\theta) = P^{\text{set}}$. Since P^{set} is γ-feasible, θ^* is well defined in $\overline{\Delta}_G(\gamma)$. By the reasoning leading to Theorem 3.2 (see [16, Theorem 2]), the shifted system (11) is stable if and only if all D_i are nonnegative. ■

Remark 2: **(Generation Constraints).** For a γ-feasible injection setpoint, the inverter generation constraint $P_i^{\text{set}} \in [0, \overline{P}_i]$ is generally not met. This constraint is feasible if $P_i^* = 0$ ($i \in \mathcal{V}_I$) and an additional parametric condition holds:

$$-\sum\nolimits_{j\in\mathcal{V}_L} P_j^* \leq \left(\overline{P}_i/D_i\right)\sum\nolimits_{j\in\mathcal{V}_I} D_j \,, \quad i \in \mathcal{V}_I \,. \tag{18}$$

The inequalities (18) limit the heterogeneity of the inverter power injections, and are sufficient for the load serviceability condition (3), as one can see by rearranging and summing over all $i \in \mathcal{V}_I$. A similar result holds for the choice $P_i^* = \overline{P}_i$. □

IV. Centralized, Decentralized, and Distributed Secondary Control Strategies

The primary droop controller (4) results in the static frequency error ω_{sync} in (5). The purpose of the secondary control $u_i(t)$ in (6) is to eliminate this frequency error despite unknown and variable loads. In this section, we investigate different decentralized and distributed secondary control strategies.

A. Decentralized Secondary Integral Control

To investigate decentralized secondary control, we partition the set of inverters as $\mathcal{V}_I = \mathcal{V}_{I_P} \cup \mathcal{V}_{I_S}$, where the action of the $\mathcal{V}_{I_P}$ inverters is restricted to primary droop control, and the $\mathcal{V}_{I_S}$ inverters use the local frequency error for integral control:

$$\begin{aligned} &u_i(t) = -p_i \;\;,\;\; k_i\dot{p}_i = \dot{\theta}_i \,, && i \in \mathcal{V}_{I_S} \,, \\ &u_i(t) = 0 \,, && i \in \mathcal{V}_{I_P} \,. \end{aligned} \tag{19}$$

Consider the case $|\mathcal{V}_{I_S}| = 1$, which mimics AGC inside a control area of a transmission network. It can be shown, as a direct corollary to Theorem 4.3 (in Section IV-D), that this controller achieves frequency regulation but fails to maintain the power sharing. Additionally, if a steady-state exists, p_i must converge to the total power imbalance $\sum_{i\in\mathcal{V}} P_i^*$, which places a large and unpredictable burden on a single generator.

For $|\mathcal{V}_{I_S}| \geq 2$, the control (19) results in a set of invariant closed-loop subspaces corresponding to different choices of u^* rendering ω_{sync}^* to zero (see (7)). One way to remove these subspaces is to implement (19) via the low-pass filter

$$u_i(t) = -p_i \;\;,\;\; k_i\dot{p}_i = \dot{\theta}_i - \epsilon p_i \,, \qquad i \in \mathcal{V}_{I_S} \,, \tag{20}$$

For small $\epsilon > 0$ and large $k > 0$ (enforcing a time-scale separation), the controller (20) achieves practical stabilization but does not exactly regulate the frequency [26]. In conclusion, the decentralized control (19) and its variations generally fail to achieve fast frequency regulation while maintaining power sharing among generating units. Additionally, a single microgrid source may not have the authority or the capacity to perform secondary control. In the following, we analyze distributed strategies that exactly recover the primary injections.

B. Centralized Averaging PI (CAPI) Control

Different distributed secondary control strategies have been proposed in [24], [25]. In [24], an integral feedback of a *weighted average frequency* among all inverters is proposed:[3]

$$u_i(t) = -p_i \quad , \quad k_i \dot{p}_i = \frac{\sum_{j \in \mathcal{V}_I} D_j \dot{\theta}_j}{\sum_{j \in \mathcal{V}_I} D_j} \, , \quad i \in \mathcal{V}_I \, , \tag{21}$$

Here, p_i is the secondary variable and $k_i > 0$. For $P_i^* = 0$, the average frequency in (21) is the sum of the inverter injections $P_{\mathrm{e},i}(\theta)$. In this case, (21) equals the secondary control strategy in [25], where the averaged inverter injections are integrated.

By counter-examples, it can be shown that the secondary controller (21) does not have the power sharing property of the shifted control system (11) unless the values of D_i and k_i are carefully tuned. In the following, we suggest the choice

$$k_i = k/D_i \, , \quad i \in \mathcal{V}_I \, , \tag{22}$$

where $k > 0$. The closed loop (2), (6), (21), (22) is given by

$$0 = P_i^* - P_{\mathrm{e},i}(\theta) \, , \qquad i \in \mathcal{V}_L \, , \tag{23a}$$

$$D_i \dot{\theta}_i = P_i^* - P_{\mathrm{e},i}(\theta) - p_i \, , \qquad i \in \mathcal{V}_I \, , \tag{23b}$$

$$k \frac{\dot{p}_i}{D_i} = \frac{\sum_{j \in \mathcal{V}_I} D_j \dot{\theta}_j}{\sum_{j \in \mathcal{V}_I} D_j} \, , \qquad i \in \mathcal{V}_I \, . \tag{23c}$$

By changing variables $q_i \triangleq p_i/D_i - \omega_{\mathrm{sync}}$ for $i \in \mathcal{V}_I$ and observing that $k\dot{q}_i = \sum_{j \in \mathcal{V}_I} D_j \dot{\theta}_j / \sum_{j \in \mathcal{V}_I} D_j$ is identical for all $i \in \mathcal{V}_I$, we can rewrite the closed-loop equations (23) as

$$0 = \widetilde{P}_i - P_{\mathrm{e},i}(\theta) \, , \qquad i \in \mathcal{V}_L \, , \tag{24a}$$

$$D_i \dot{\theta}_i = \widetilde{P}_i - P_{\mathrm{e},i}(\theta) - D_i q \, , \qquad i \in \mathcal{V}_I \, , \tag{24b}$$

$$k \dot{q} = \frac{\sum_{j \in \mathcal{V}_I} D_j \dot{\theta}_j}{\sum_{j \in \mathcal{V}_I} D_j} \, , \tag{24c}$$

where $\widetilde{P}_i$ is as in (11). In this transformed system, (24c) can be implemented as a *centralized controller*: it receives information from all inverters and then dispatches the secondary control variable q. Due to this insight on the controller's communication complexity, we refer to (21)-(22) as the *centralized averaging proportional integral* (CAPI) controller.

Theorem 4.1: **(Stability of CAPI-Controlled Network).** Consider the droop-controlled microgrid (2),(6) with $P_i^* \in [0, \overline{P}_i]$ and $D_i > 0$ for $i \in \mathcal{V}_I$. Assume a complete communication topology among the inverters $\mathcal{V}_I$, and let $u_i(t)$ be given by the CAPI controller (21) with the parametric choice (22). The following two statements are equivalent:

(i) ***Stability of primary droop control:*** the droop control stability condition (14) holds;

(ii) ***Stability of CAPI control:*** there exists an arc length $\gamma \in [0, \pi/2[$ such that the closed loop (23) possesses a locally exponentially stable and unique equilibrium manifold $([\theta^*], p^*) \subset \overline{\Delta}_G(\gamma) \times \mathbb{R}^{n_I}$.

If the equivalent statements (i) and (ii) hold true, then $[\theta^*]$ is given as in Theorem 3.2, and $p_i^* = D_i \omega_{\mathrm{sync}}$ for $i \in \mathcal{V}_I$.

Proof: We start by writing system (24) in vector form. Let $D_I = \mathrm{diag}(\{D_i\}_{i \in \mathcal{V}_I})$, and let $D_{\mathrm{tot}} = \sum_{i \in \mathcal{V}_I} D_i$. Let $\widetilde{P} = (\widetilde{P}_L, \widetilde{P}_I)$, and accordingly let $P_{\mathrm{e}}(\theta) = (P_{\mathrm{e},L}(\theta), P_{\mathrm{e},I}(\theta))$, where $P_{\mathrm{e},I}(\theta)$ and $P_{\mathrm{e},L}(\theta)$ are the injections for nodes $\mathcal{V}_I$ and $\mathcal{V}_L$. Accordingly, partition the angles as $\theta = (\theta_L, \theta_I)$. With this notation, the closed loop (24) reads in vector form as

$$\underbrace{\begin{bmatrix} I & \mathbf{0} & \mathbf{0} \\ \mathbf{0} & D_I & \mathbf{0} \\ \mathbf{0} & \mathbf{0} & k \cdot D_{\mathrm{tot}} \end{bmatrix}}_{\triangleq Q_1} \begin{bmatrix} \mathbf{0} \\ \dot{\theta}_I \\ \dot{q} \end{bmatrix} = \begin{bmatrix} I & \mathbf{0} & \mathbf{0} \\ \mathbf{0} & I & D_I \mathbf{1} \\ \mathbf{0} & \mathbf{1}^T & D_{\mathrm{tot}} \end{bmatrix} \begin{bmatrix} \widetilde{P}_L - P_{\mathrm{e},L}(\theta) \\ \widetilde{P}_I - P_{\mathrm{e},I}(\theta) \\ -q \end{bmatrix}$$

$$= \underbrace{\begin{bmatrix} I & \mathbf{0} & \mathbf{0} \\ \mathbf{0} & D_I & \mathbf{0} \\ \mathbf{0} & \mathbf{0} & 1 \end{bmatrix}}_{\triangleq Q_2} \underbrace{\begin{bmatrix} I & \mathbf{0} & \mathbf{0} \\ \mathbf{0} & D_I^{-1} & \mathbf{1} \\ \mathbf{0} & \mathbf{1}^T & D_{\mathrm{tot}} \end{bmatrix}}_{\triangleq Q_3} \underbrace{\begin{bmatrix} \widetilde{P}_L - P_{\mathrm{e},L}(\theta) \\ \widetilde{P}_I - P_{\mathrm{e},I}(\theta) \\ -q \end{bmatrix}}_{\triangleq x} . \tag{25}$$

The matrices Q_1 and Q_2 are nonsingular, while Q_3 is singular with $\ker(Q_3) = \mathrm{Span}\left([0\,, (D_I \mathbf{1}_{n_I})\,, -1]\right)$. On the other hand, $[\mathbf{1}_n^T \; \mathbf{1}_n^T \; 0]x = 0$ due to balanced injections $\mathbf{1}^T \widetilde{P} = 0$ and flows $\mathbf{1}^T P_{\mathrm{e}}(\theta) = 0$. It follows that $x \notin \ker(Q_3)$. Thus, possible equilibria of (25) are $x = \mathbf{0}_n$, that is, the equilibria $[\theta^*]$ from (11) and $q^* = 0$. By Theorem 3.2, the equation $x = \mathbf{0}_n$ is solvable for $[\theta^*] \in \overline{\Delta}_G(\gamma)$ if and only if condition (14) holds.

To establish stability, observe that the negative power flow Jacobian $-\partial P_{\mathrm{e}}(\theta)/\partial\theta$ equals the Laplacian matrix $\mathcal{L}(\theta) = B^T \mathrm{diag}(\{a_{ij}\}_{\{i,j\} \in \mathcal{E}}) B$ with $a_{ij} \triangleq \mathfrak{Im}(Y_{ij}) E_i E_j \cos(\theta_i - \theta_j)$ as weights [30, Lemma 2]. For $[\theta^*] \in \overline{\Delta}_G(\gamma)$, all weights $a_{ij} > 0$ are strictly positive for $\{i, j\} \in \mathcal{E}$, and $\mathcal{L}(\theta^*)$ is a positive semidefinite Laplacian. A linearization of the DAE (25) about the regular set of fixed points $([\theta^*], 0)$ and elimination of the algebraic variables gives the reduced Jacobian

$$J(\theta^*) = \underbrace{\begin{bmatrix} I & \mathbf{0} \\ \mathbf{0} & (k \cdot D_{\mathrm{tot}})^{-1} \end{bmatrix}}_{\triangleq \widetilde{Q}_1} \underbrace{\begin{bmatrix} D_I^{-1} & \mathbf{1} \\ \mathbf{1}^T & D_{\mathrm{tot}} \end{bmatrix}}_{\triangleq \widetilde{Q}_2} \underbrace{\begin{bmatrix} -\mathcal{L}_{\mathrm{red}}(\theta^*) & \mathbf{0} \\ \mathbf{0} & -1 \end{bmatrix}}_{\triangleq X} ,$$

where $\mathcal{L}_{\mathrm{red}}(\theta^*)$ is the Schur complement of $\mathcal{L}(\theta^*)$ with respect to the load entries with indices $\mathcal{V}_I$. It is known that $\mathcal{L}_{\mathrm{red}}(\theta^*)$ is again a positive semidefinite Laplacian [35, Lemma II.1]. The matrix $\widetilde{Q}_1$ is diagonal and positive definite, and $\widetilde{Q}_2$ is positive semidefinite with $\ker(\widetilde{Q}_2) = \mathrm{Span}\left([(D_I \mathbf{1}_{n_I})\,, -1]\right)$.

We proceed via a continuity-type argument. Consider momentarily the perturbed Jacobian $J_\epsilon(\theta^*)$, where $\widetilde{Q}_2$ is replaced by the positive definite matrix $\widetilde{Q}_{2,\epsilon} = \left[\begin{smallmatrix} D_I^{-1} & \mathbf{1} \\ \mathbf{1}^T & D_{\mathrm{tot}} + \epsilon \end{smallmatrix}\right]$ with $\epsilon > 0$. The spectrum of $J_\epsilon(\theta^*)$ is obtained from $\widetilde{Q}_1 \widetilde{Q}_{2,\epsilon} X v = \lambda v$ for

[3] The controller [24] also contains a proportional feedback of the average frequency. We found that such a proportional feedback does not preserve the equilibria of the shifted control system (11) (unless the gains are carefully tuned), and we omit it here. The controller in [24] uses an arithmetic average with all $D_i = 1$ in (21). Since the synchronization frequency (5) is obtained by a weighted average and since $D_i \dot{\theta}_i$ is the inverter injection $P_{\mathrm{e},i}(\theta)$ (for $P_i^* = 0$), we found the choice (21) more natural. Simulations indicate that any convex combination of the inverter frequencies yields identical results.

some $(\lambda, v) \in \mathbb{C} \times \mathbb{C}^{n_I+1}$. Equivalently, let $y = \widetilde{Q}_1^{-1} v$, then

$$-\widetilde{Q}_{2,\epsilon} \cdot \mathrm{blkdiag}(\mathcal{L}_{\mathrm{red}}\,,\, 1/(k \cdot D_{\mathrm{tot}}))\, y = \lambda y\,.$$

The Courant-Fischer Theorem applied to this generalized eigenvalue problem implies that, for $\epsilon > 0$ and modulo rotational symmetry, all eigenvalues λ are real and negative.

Now, consider again the unperturbed case with $\epsilon = 0$. Recall that $\ker(\widetilde{Q}_2) = \mathrm{Span}\left([(D_I \mathbf{1}_{n_I})\,, -1]\right)$, and the image of the matrix $\mathrm{blkdiag}(\mathcal{L}_{\mathrm{red}}\,,\, 1/(k \cdot D_{\mathrm{tot}}))$ excludes $\mathrm{Span}\left([\mathbf{1}_{n_I}\,, 0]\right)$. It follows that $\widetilde{Q}_2 \cdot \mathrm{blkdiag}(\mathcal{L}_{\mathrm{red}}\,,\, 1/(k \cdot D_{\mathrm{tot}}))\, y$ is zero if only if $y \in \mathrm{Span}([\mathbf{1}_{n_I}\,, 0])$ corresponding to the rotational symmetry. We conclude that the number of negative real eigenvalues of $J_\epsilon(\theta^*)$ does not change as $\epsilon \searrow 0$. Hence, the equilibrium $([\theta^*], 0)$ of the DAE (25) is locally exponentially stable. ■

The CAPI controller (21),(22) preserves the primary power injections while restoring the frequency. However, it requires all-to-all communication among the inverters, and a restrictive choice of gains (22). To overcome these limitations, we present an alternative controller and a modification of CAPI control.

C. Distributed Averaging PI (DAPI) Control

As third secondary control strategy, consider the *distributed averaging proportional integral* (DAPI) controller [16]:

$$u_i = -p_i\ ,\ k_i \dot{p}_i = D_i \dot{\theta}_i + \sum\nolimits_{j \in \mathcal{V}_I} L_{ij} \left(\frac{p_i}{D_i} - \frac{p_j}{D_j} \right). \quad (26)$$

Here, $k_i > 0$ and L is the Laplacian matrix of a weighted, connected and undirected communication graph between the inverters. The resulting closed-loop system is then given by

$$\begin{aligned} 0 &= P_i^* - P_{\mathrm{e},i}(\theta)\,, && i \in \mathcal{V}_L\,, && (27\mathrm{a})\\ D_i \dot{\theta}_i &= P_i^* - P_{\mathrm{e},i}(\theta) - p_i\,, && i \in \mathcal{V}_I\,, && (27\mathrm{b})\\ k_i \dot{p}_i &= D_i \dot{\theta}_i + \sum\nolimits_{j \in \mathcal{V}_I} L_{ij} \left(\frac{p_i}{D_i} - \frac{p_j}{D_j} \right), && i \in \mathcal{V}_I\,. && (27\mathrm{c}) \end{aligned}$$

The following result has been established in earlier work [16, Theorem 8] and shows the stability of the closed loop (27).

Theorem 4.2: **(Stability of DAPI-Controlled Network).** Consider the droop-controlled microgrid (2),(6) with parameters $P_i^* \in [0, \overline{P}_i]$, and $D_i > 0$ for $i \in \mathcal{V}_I$. Let the secondary control inputs be given by (26) with $k_i > 0$ for $i \in \mathcal{V}_I$ and a connected communication graph among the inverters $\mathcal{V}_I$ with Laplacian L. The following two statements are equivalent:

(i) ***Stability of primary droop control:*** the droop control stability condition (14) holds;

(ii) ***Stability of secondary integral control:*** there exists an arc length $\gamma \in [0, \pi/2[$ such that the closed loop (23) possesses a locally exponentially stable and unique equilibrium manifold $([\theta^*], p^*) \subset \overline{\Delta}_G(\gamma) \times \mathbb{R}^{n_I}$.

If the equivalent statements (i) and (ii) hold true, then $[\theta^*]$ is given as in Theorem 3.2, and $p_i^* = D_i \omega_{\mathrm{sync}}$ for $i \in \mathcal{V}_I$.

The DAPI control (26) regulates the network frequency, requires only a sparse communication network, and preserves the power injections established by primary control. Moreover, the gains $D_i > 0$ and $k_i > 0$ can be chosen independently.

We remark that a higher-order variation of the DAPI control (26) (additionally integrating edge flows) can also be derived from a network flow optimization perspective [15], [36].

D. Partial Secondary Control

The DAPI and CAPI controller require that *all* inverters participate in secondary control. To further reduce the communication complexity and increase the adaptivity of the microgrid, it is desirable that only a subset of inverters regulate the frequency. To investigate this scenario, we partition the set of inverters as $\mathcal{V}_I = \mathcal{V}_{I_P} \cup \mathcal{V}_{I_S}$, where the action of the $\mathcal{V}_{I_P}$ inverters is restricted to primary droop control, and the $\mathcal{V}_{I_S}$ inverters perform the secondary DAPI or CAPI control:

$$\begin{aligned} D_i \dot{\theta}_i &= P_i^* - P_{\mathrm{e},i}(\theta)\,, && i \in \mathcal{V}_{I_P}\,, && (28\mathrm{a})\\ D_i \dot{\theta}_i &= P_i^* - P_{\mathrm{e},i}(\theta) + u_i(t)\,, && i \in \mathcal{V}_{I_S}\,, && (28\mathrm{b}) \end{aligned}$$

Observe that the $\mathcal{V}_{I_P}$ inverters are essentially frequency-dependent loads and the previous analysis applies. The following result shows that partial secondary control strategies successfully stabilize the microgrid and regulate the frequency.

Theorem 4.3: **(Partially Regulated Networks).** Consider the droop-controlled microgrid with primary and partial secondary control (2),(28) and with parameters $P_i^* \in [0, \overline{P}_i]$, and $D_i > 0$ for $i \in \mathcal{V}_I$. For $i \in \mathcal{V}_{I_S}$, let the secondary control inputs be given by the CAPI controller (21), (22) with $|\mathcal{V}_{I_S}| \geq 1$ and a complete communication graph among the $\mathcal{V}_{I_S}$ nodes (respectively, by the DAPI controller (26) with $|\mathcal{V}_{I_S}| \geq 2$ and a connected communication graph among the $\mathcal{V}_{I_S}$ nodes). The following statements are equivalent:

(i) ***Stability of primary droop control:*** the droop control stability condition (14) holds;

(ii) ***Stability of partial secondary control:*** there is an arc length $\gamma \in [0, \pi/2[$ so that the partially regulated CAPI system (2), (21), (22), (28) (resp. DAPI system (2), (26), (28)) possesses a locally exponentially stable and unique equilibrium manifold $([\theta^*], p^*) \subset \overline{\Delta}_G(\gamma) \times \mathbb{R}^{|\mathcal{V}_{I_S}|}$.

If the equivalent statements (i) and (ii) hold true, then for $i \in \mathcal{V}_{I_S}$, $P_{\mathrm{e},i}(\theta^*)$ is given as in Theorem 3.2 and $p_i^* = D_i \omega_{\mathrm{partial}}$, where $\omega_{\mathrm{partial}} = \sum_{i \in \mathcal{V}} P_i^* / (\sum_{i \in \mathcal{V}_{I_S}} D_i)$. For all other inverters $i \in \mathcal{V}_{I_P}$, we have that $P_{\mathrm{e},i}(\theta^*) = P_i^*$.

Proof: The proof for partial CAPI control (respectively, partial DAPI control) is analogous to the proof of Theorem 4.1 (respectively, [16, Theorem 8]), while accounting for the partition $\mathcal{V}_I = \mathcal{V}_{I_P} \cup \mathcal{V}_{I_S}$ in the Jacobian matrices. ■

We now investigate the power sharing properties of partial secondary control. The steady-state injections at $([\theta^*], p^*)$ are

$$\begin{aligned} P_{\mathrm{e},i}(\theta^*) &= P_i^*, && i \in \mathcal{V}_{I_P} \cup \mathcal{V}_L\,,\\ P_{\mathrm{e},i}(\theta^*) &= P_i^* - D_i \omega_{\mathrm{partial}}, && i \in \mathcal{V}_{I_S}\,, \end{aligned}$$

By applying Theorem 3.3, we obtain the following corollary:

Corollary 4.4: **(Injection Constraints and Power Sharing with Partial Regulation).** Consider a locally exponentially stable equilibrium $([\theta^*], p^*) \subset \overline{\Delta}_G(\gamma) \times \mathbb{R}^{|\mathcal{V}_{I_S}|}$, $\gamma \in [0, \pi/2[$, of the partial secondary control system (2),(28) as in Theorem 4.3. Select the droop coefficients and injection setpoints proportionally. The following statements are equivalent:

(i) ***Injection constraints:*** $0 \leq P_{\mathrm{e},i}(\theta^*) \leq \overline{P}_i, \quad \forall i \in \mathcal{V}_{I_S}$;

(ii) ***Serviceable load:*** $0 \leq -\sum_{j \in \mathcal{V}_{I_P} \cup \mathcal{V}_L} P_j^* \leq \sum_{j \in \mathcal{V}_{I_S}} \overline{P}_j\,.$

Moreover, the inverters $\mathcal{V}_{I_S}$ performing secondary control share the load proportionally according to their power ratings.

V. Decentralized Tertiary Control Strategies

In this section, we examine the tertiary control layer. Similar to load sharing or flow shaping, we show that the AC economic dispatch (8) can be minimized by decentralized droop control.

A. Convex Reformulation of the AC Economic Dispatch

The main complication in solving the AC economic dispatch optimization (8) is the nonlinearity and nonconvexity of the AC injections constraints (1a). In practical power system operation, the nonlinear AC injection $P_{\mathrm{e}}(\theta)$ is often approximated by the linear *DC injection* $P_{\mathrm{DC}}(\theta)$ with components

$$P_{\mathrm{DC},i}(\theta) = \sum\nolimits_{j=1}^{n} \Im\mathfrak{m}(Y_{ij}) E_i E_j (\theta_i - \theta_j)\,, \qquad i \in \mathcal{V}\,. \quad (29)$$

Accordingly, the AC economic dispatch (8) is approximated by the corresponding *DC economic dispatch* given by

$$\begin{aligned} &\underset{\delta\in\mathbb{R}^n,\, v\in\mathbb{R}^{n_I}}{\text{minimize}} && f(v) = \sum\nolimits_{i\in\mathcal{V}_I} \frac{1}{2}\alpha_i v_i^2 && && (30\text{a})\\ &\text{subject to} && P_i^* + v_i = P_{\mathrm{DC},i}(\delta) && \forall\, i \in \mathcal{V}_I\,, && (30\text{b})\\ & && P_i^* = P_{\mathrm{DC},i}(\delta) && \forall\, i \in \mathcal{V}_L\,, && (30\text{c})\\ & && |\delta_i - \delta_j| \le \gamma_{ij}^{(\mathrm{DC})} && \forall\, \{i,j\} \in \mathcal{E}\,, && (30\text{d})\\ & && P_{\mathrm{DC},i}(\delta) \in [0, \overline{P}_i] && \forall\, i \in \mathcal{V}_I\,, && (30\text{e}) \end{aligned}$$

where (δ, v) are the DC variables are distinguished from the AC variables (θ, u). In formulating the DC economic dispatch (30), we also changed the line flow parameters from $\gamma_{ij}^{(\mathrm{AC})}$ to $\gamma_{ij}^{(\mathrm{DC})} \in [0, \pi/2[$ for all $\{i,j\} \in \mathcal{E}$. The DC dispatch (30) is a quadratic program with linear constraints and hence convex.

Typically, the solution (δ^*, v^*) of the DC dispatch (30) serves as proxy for the solution of the non-convex AC dispatch (8). The following result shows that both problems are equivalent for acyclic networks and appropriate security constraints.

Theorem 5.1: **(Equivalence of AC and DC Economic Dispatch in Acyclic Networks).** Consider the AC economic dispatch (8) and the DC economic dispatch (30) in an acyclic network. The following statements are equivalent:

(i) ***AC feasibility:*** the AC economic dispatch problem (8) with parameters $\gamma_{ij}^{(\mathrm{AC})} < \pi/2$ for all $\{i,j\} \in \mathcal{E}$ is feasible with a global minimizer $(\theta^*, u^*) \in \mathbb{T}^n \times \mathbb{R}^{n_I}$;

(ii) ***DC feasibility:*** the DC economic dispatch problem (30) with parameters $\gamma_{ij}^{(\mathrm{DC})} < 1$ for all $\{i,j\} \in \mathcal{E}$ is feasible with a global minimizer $(\delta^*, v^*) \in \mathbb{R}^n \times \mathbb{R}^{n_I}$.

If the equivalent statements (i) and (ii) are true, then $\sin(\gamma_{ij}^{(\mathrm{AC})}) = \gamma_{ij}^{(\mathrm{DC})}$, $u^* = v^*$, $\mathbf{sin}(B^T\theta^*) = B^T\delta^*$, and $f(u^*) = f(v^*)$ is a global minimum.

Proof: Denote the unique vector of AC branch power flows by $\xi = \mathcal{A}\,\mathbf{sin}(B^T\theta)$; see (13). For an acyclic network, we have $\ker(B) = \emptyset$, and $\xi \in \mathbb{R}^{n-1}$ can be equivalently rewritten as $\xi = \mathcal{A}B^T\delta$ for some $\delta \in \mathbb{R}^n$. Thus, we obtain

$$\mathcal{A}\,\mathbf{sin}(B^T\theta) = \mathcal{A}B^T\delta\,. \quad (31)$$

Now, we associate δ with the angles of the DC flow (29), so that (31) is a *bijective map* between the AC and the DC flows.

Due to the AC security constraints (8d), the sine function is invertible. If the DC security constraints (30d) satisfy $\|B^T\delta\|_\infty \le \max_{\{i,j\}\in\mathcal{E}} \gamma_{ij}^{(\mathrm{DC})} < 1$, then $B^T\theta$ can be uniquely recovered from (and mapped to) $B^T\delta$ via (31). Additionally, up to rotational symmetry and modulo 2π, the angle θ and be uniquely recovered from (and mapped to) δ. Thus, identity (31) between the AC and the DC flow serves as a *bijective change of variables* (modulo 2π and up to rotational symmetry).

This change of variables maps the AC economic dispatch (8) to the DC economic dispatch (30) as follows. The AC injections $P_{\mathrm{e}}(\theta)$ are replaced by the DC injections $P_{\mathrm{DC}}(\delta)$. The AC security constraint (8d) translates uniquely to the DC constraint (30d) with $\gamma_{ij}^{(\mathrm{DC})} = \sin(\gamma_{ij}^{(\mathrm{AC})}) < 1$. The AC injection constraint (8e) is mapped to the DC injection constraint (30e).

Finally, if both problems (8) and (30) are feasible with minimizers $u^* = v^*$ and $\mathbf{sin}(B^T\theta^*) = B^T\delta^*$, then $f(u^*) = f(v^*)$ is the unique global minimum due to convexity of (30). ■

Theorem 5.1 relies on the bijection (31) between AC and DC flows in acyclic networks [30], [31]. For cyclic networks, the two problems (8) and (30) are generally not equivalent, but the DC flow is a well-accepted proxy for the AC flow.

We now state a rather surprising result: any minimizer of the AC economic dispatch (8) can be achieved by an appropriately designed droop control (4). Conversely, any steady state of the droop-controlled microgrid (2),(4) is the minimizer of an AC economic dispatch (8) with appropriately chosen parameters. The following theorem makes this idea precise for strictly feasible minimizers (which strictly satisfying the inequality constraints) and strictly positive (stabilizing) droop coefficients. The proof can be easily extended to the constrained case at the cost of a less explicit relation between the optimization parameters and the (possibly non-positive) droop coefficients.

Theorem 5.2: **(Droop Control & Economic Dispatch).** Consider the AC economic dispatch (8) and the shifted control system (11). The following statements are equivalent:

(i) ***Strict feasibility and optimality:*** there are parameters $\alpha_i > 0$, $i \in \mathcal{V}_I$, and $\gamma_{ij}^{(\mathrm{AC})} < \pi/2$, $\{i,j\} \in \mathcal{E}$ such that the AC economic dispatch problem (8) is strictly feasible with global minimizer $(\theta^*, u^*) \in \mathbb{T}^n \times \mathbb{R}^{n_I}$.

(ii) ***Constrained synchronization:*** there exists $\gamma \in [0, \pi/2[$ and droop coefficients $D_i > 0$, $i \in \mathcal{V}_I$, so that the shifted control system (11) possesses a unique and locally exponentially stable equilibrium manifold $[\theta] \subset \Delta_G(\gamma)$ meeting the injection constraints $P_{\mathrm{e},i}(\theta) \in]0, \overline{P}_i[, i \in \mathcal{V}_I$.

If the equivalent statements (i) and (ii) hold true, then $[\theta^*] = [\theta]$, $\gamma = \max_{\{i,j\}\in\mathcal{E}} \gamma_{ij}^{(\mathrm{AC})}$, and for some $\beta > 0$ it holds that

$$D_i = \beta/\alpha_i\,, \qquad i \in \mathcal{V}_I\,. \quad (32)$$

Theorem 5.2, stated for the shifted control system (11), can be equivalently stated for the CAPI or DAPI control systems (by Lemma 3.1). Before proving it, we state a key lemma.

Lemma 5.3: **(Properties of strictly feasible points).** If $(\theta^*, u^*) \in \mathbb{T}^n \times \mathbb{R}^{n_I}$ is a strictly feasible minimizer of the AC economic dispatch (8), then u^* is *sign-definite*, that is, all u_i^*, $i \in \mathcal{V}_I$, have the same sign. Conversely, any strictly feasible pair $(\theta, u) \in \mathbb{T}^n \times \mathbb{R}^{n_I}$ of the AC economic dispatch (8) with sign-definite u is *inverse optimal* with respect to some $\alpha \in \mathbb{R}^{n_I}_{>0}$: there is a set of coefficients $\alpha_i > 0$, $i \in \mathcal{V}_I$, such that (θ, u) is global minimizer of the AC economic dispatch (8).

Proof: The strictly feasible pairs of (8) are given by the set of all $(\theta, u) \in \mathbb{T}^n \times \mathbb{R}^{n_I}$ satisfying the power flow equations (8b)-(8c) and the strict inequality constraints (8d)-(8e). Summing all equations (8b)-(8c) yields the necessary solvability condition (power balance constraint) $\sum_{i\in\mathcal{V}_I} u_i = -\sum_{i\in\mathcal{V}} P_i^*$.

To establish the necessary and sufficient optimality conditions for (8) in the strictly feasible case, without loss of generality, we drop the inequality constraints (8d)-(8e). With $\lambda \in \mathbb{R}^n$, the Lagrangian $\mathcal{L} : \mathbb{T}^n \times \mathbb{R}^{n_I} \times \mathbb{R}^n \to \mathbb{R}$ is given by

$$\mathcal{L}(\theta, u, \lambda) = \sum_{j\in\mathcal{V}_I} \frac{1}{2}\alpha_j u_j^2 + \sum_{j\in\mathcal{V}_I} \lambda_j \left(u_j + P_j^* - P_{\mathrm{e},j}(\theta)\right) + \sum_{j\in\mathcal{V}_L} \lambda_j \left(P_j^* - P_{\mathrm{e},j}(\theta)\right) .$$

The necessary KKT conditions [37] for optimality are:

$$\frac{\partial\mathcal{L}}{\partial\theta_i} = 0 \;:\; 0 = \sum_{j\in\mathcal{V}} \lambda_j \cdot \frac{\partial P_{\mathrm{e},j}(\theta)}{\partial\theta_i}\,, \quad \forall i \in \mathcal{V}\,, \tag{33a}$$

$$\frac{\partial\mathcal{L}}{\partial u_i} = 0 \;:\; \alpha_i u_i = -\lambda_i\,, \quad \forall i \in \mathcal{V}_I\,, \tag{33b}$$

$$\frac{\partial\mathcal{L}}{\partial\lambda_i} = 0 \;:\; -u_i = P_i^* - P_{\mathrm{e},i}(\theta)\,, \quad \forall i \in \mathcal{V}_I\,, \tag{33c}$$

$$\frac{\partial\mathcal{L}}{\partial\lambda_i} = 0 \;:\; 0 = P_i^* - P_{\mathrm{e},i}(\theta)\,, \quad \forall i \in \mathcal{V}_L\,. \tag{33d}$$

Since the AC economic dispatch (8) is equivalent to the convex DC dispatch (see Theorem 5.1), the KKT conditions (33) are also sufficient for optimality. In vector form, (33a) reads as $\mathbf{0}_n = \lambda^\mathsf{T}\partial P_{\mathrm{e}}(\theta)/\partial\theta$, where the *load flow Jacobian* is given by symmetric Laplacian $\partial P_{\mathrm{e}}(\theta)/\partial\theta = B^T \operatorname{diag}(\{a_{ij}\}_{\{i,j\}\in\mathcal{E}})B$ with strictly positive weights $a_{ij} = \mathfrak{Im}(Y_{ij})E_iE_j\cos(\theta_i - \theta_j)$ (due to strict feasibility of the security constraint (8d)). It follows that $\lambda \in \mathbb{1}_n$, that is, $\lambda_i = \widetilde{\lambda} \in \mathbb{R}$ for all $i \in \mathcal{V}$ and for some $\widetilde{\lambda} \in \mathbb{R}$. Hence, condition (33b) reads as $u_i = -\widetilde{\lambda}/\alpha_i$ for all $i \in \mathcal{V}_I$, and the conditions (33c)-(33d) reduce to

$$\widetilde{\lambda}/\alpha_i = P_i^* - P_{\mathrm{e},i}(\theta)\,, \quad \forall i \in \mathcal{V}_I\,, \tag{34a}$$

$$0 = P_i^* - P_{\mathrm{e},i}(\theta)\,, \quad \forall i \in \mathcal{V}_L\,. \tag{34b}$$

By summing all equations (34), we obtain the constant $\widetilde{\lambda}$ as $\widetilde{\lambda} = \sum_{i\in\mathcal{V}} P_i^* / \sum_{i\in\mathcal{V}_\mathcal{I}} \alpha_i^{-1}$. The minimizers are $u_i^* = -\widetilde{\lambda}/\alpha_i$ and θ^* determined from (34). It follows that u^* is sign-definite.

By comparing the (strict) optimality conditions (34) with the (strict) feasibility conditions (8b)-(8c), it follows that any strictly feasible pair (θ, u) with sign-definite u is inverse optimal for the coefficients $\alpha_i = -\beta/u_i$ with some $\beta > 0$. ■

Proof of Theorem 5.2: **(i) $\implies$ (ii):** If the AC economic dispatch (8) is strictly feasible, then its minimizer (θ^*, u^*) is global (Theorem 5.1), and the optimal inverter injections are $P_i^{\mathrm{opt}} = P_{\mathrm{e},i}(\theta^*) = P_i^* + u_i^*$ with sign-definite u^* (Lemma 5.3). Since the power flow equations (8b)-(8c) and the strict inequality constraints (8d)-(8e) are met, $P_i^{\mathrm{opt}} \in \,]0, \overline{P}_i[$, $[\theta^*] \subset \Delta_G(\gamma)$ with $\gamma = \max_{\{i,j\}\in\mathcal{E}} \gamma_{ij}^{(\mathrm{AC})}$, and the vector of load and source injections $(P_L^*, P_I^{\mathrm{opt}})$ is a γ-feasible injection setpoint.

By Theorem 3.4 and identity (17), the droop coefficients $D_i = -\beta(P_i^* - P_i^{\mathrm{opt}}) = \beta u_i^*$, $i \in \mathcal{V}_I$, guarantee that the shifted control system (11) possesses an equilibrium manifold $[\theta]$ satisfying $P_{\mathrm{e}}(\theta) = P^{\mathrm{set}} = P_{\mathrm{e}}(\theta^*)$. For $\beta u_i^* > 0$ (recall u^* is sign-definite), $[\theta]$ is locally exponentially stable by Theorem 3.2. Finally, the identity $P_{\mathrm{e}}(\theta) = P_{\mathrm{e}}(\theta^*)$ shows that $[\theta^*] = [\theta]$.

(ii) $\implies$ (i): Any equilibrium manifold $[\theta] \subset \Delta_G(\gamma)$ as in (ii) is a γ-feasible power injection setpoint with

$$\widetilde{P}_i = P_i^* - D_i\omega_{\mathrm{sync}} = P_{\mathrm{e},i}(\theta) \quad \forall\, i \in \mathcal{V}_I\,, \tag{35a}$$

$$\widetilde{P}_i = P_i^* = P_{\mathrm{e},i}(\theta) \quad \forall\, i \in \mathcal{V}_L\,, \tag{35b}$$

$$|\theta_i - \theta_j| < \gamma \quad \forall\, i,j \in \mathcal{E}\,, \tag{35c}$$

$$P_{\mathrm{e},i}(\theta) \in \,]0, \overline{P}_i[\quad \forall\, i \in \mathcal{V}_I\,. \tag{35d}$$

Hence, any $\theta \in [\theta]$ is strictly feasible for the economic dispatch (8) if we identify θ^* with θ (modulo symmetry), γ with $\max_{\{i,j\}\in\mathcal{E}} \gamma_{ij}^{(\mathrm{AC})}$, and u_i^* with $-D_i\omega_{\mathrm{sync}}$ (modulo scaling). Since u_i^* is sign-definite, the claim follows from Lemma 5.3.

In the strictly feasible case, a comparison of the stationarity conditions (35a)-(35b) and the optimality conditions (34) gives $D_i\omega_{\mathrm{sync}} = -u_i^* = \widetilde{\lambda}/\alpha_i$, where ω_{sync} and $\widetilde{\lambda}$ are constant. Since the droop gains are defined up to scaling, we obtain (32). ■

The equivalence revealed in Theorem 5.2 suggests the following guidelines to select the droop coefficients: large coefficients D_i for desirable (e.g., economic or low emission) sources with small marginal costs α_i; and vice versa. These insights can also be connected to the proportional power sharing objective: if each P_i^* and $1/\alpha_i$ are selected proportional to the rating $\overline{P}_i$, that is, $\alpha_i\overline{P}_i = \alpha_j\overline{P}_j$ and $P_i^*/\overline{P}_i = P_j^*/\overline{P}_j$, then the associated droop coefficients (32) equal those in (16).

From an optimization perspective, the primary dynamics (11) serve as a primal algorithm to minimize (8). Likewise, second-order or integral control dynamics serve as primal-dual algorithm, as shown for related systems in [13]–[15], [36]

VI. Simulation Case Study

We illustrate the performance and robustness of our controllers via simulation of the lossy IEEE 37 distribution system shown in Fig. 1(a). After an islanding event, the distribution network is disconnected from the transmission grid, and distributed generators must ensure stability while regulating the frequency and sharing the demand. The cyber layer describing the communication among the distributed generators is shown in dotted blue. Of the 16 sources, 8 have identical power ratings, while the other 8 are rated for twice as much power.

Instead of the lossless power flow (1), we use the lossy equations [9]. To include reactive power dynamics, the inverter voltages are controlled via the *quadratic voltage-droop* [17]

$$\tau_i\dot{E}_i = -C_iE_i(E_i - E_i^*) - Q_{\mathrm{e},i}, \quad i \in \mathcal{V}_I\,,$$

where $E_i^* > 0$ is the nominal voltage, $C_i, \tau_i > 0$ are gains, and $Q_{\mathrm{e},i} \in \mathbb{R}$ is the reactive power injection (1b). Fig. 1(b) and (c) show a comparison between the decentralized secondary controllers (19) implemented at every inverter, and the DAPI controller (26), with equal gains. While both controllers regulate the frequency, the decentralized controllers (19) does not maintain the power sharing property under a change in load.

VII. Conclusions

We studied decentralized and distributed primary, secondary, and tertiary control strategies in microgrids and illuminated some connections between them. Thereby, we relaxed some restrictions regarding the information structure and time-scale separation of conventional hierarchical control strategies

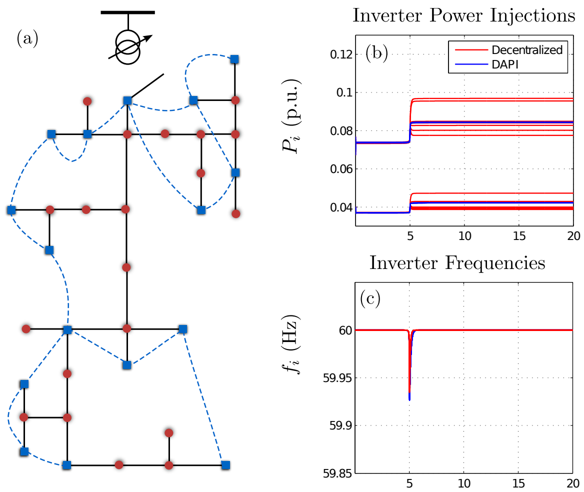

Fig. 1. Comparison of decentralized control (20) and DAPI control (26).

adapted from transmission-level networks to make them more applicable to microgrids and distribution-level applications.

While this work is a first step towards an understanding of the interdependent control loops in hierarchical microgrids, several complicating factors have not been taken into account. In particular, our analysis is thus far formally restricted to acyclic networks with lossless (or constant R/X ratio) lines. Moreover, future work needs to consider more detailed models including reactive power flows, voltage dynamics, and ramping constraints on the inverter power injections.

Acknowledgments

The authors wish to thank H. Bouattour, J. M. Guerrero, Q.-C. Zhong, A. Domínguez-García, N. Ainsworth, and M. Andreasson for insightful discussions and sharing their preprints.

References

[1] H. Bouattour, J. W. Simpson-Porco, F. Dörfler, and F. Bullo, "Further results on distributed secondary control in microgrids," in *IEEE Conf. on Decision and Control*, Florence, Italy, Dec. 2013, pp. 1514–1519.
[2] R. H. Lasseter, "Microgrids," in *IEEE Power Engineering Society Winter Meeting*, vol. 1, 2002, pp. 305–308.
[3] M. C. Chandorkar, D. M. Divan, and R. Adapa, "Control of parallel connected inverters in standalone AC supply systems," *IEEE Transactions on Industry Applications*, vol. 29, no. 1, pp. 136–143, 1993.
[4] Q.-C. Zhong and T. Hornik, *Control of Power Inverters in Renewable Energy and Smart Grid Integration*. Wiley-IEEE Press, 2013.
[5] J. M. Guerrero, J. C. Vasquez, J. Matas, L. G. de Vicuna, and M. Castilla, "Hierarchical control of droop-controlled AC and DC microgrids–a general approach toward standardization," *IEEE Transactions on Industrial Electronics*, vol. 58, no. 1, pp. 158–172, 2011.
[6] J. M. Guerrero, M. Chandorkar, T.-L. Lee, and P. Chiang Loh, "Advanced control architectures for intelligent microgrids — Part I: Decentralized and hierarchical control," *IEEE Transactions on Industrial Electronics*, vol. 60, no. 4, pp. 1254–1262, 2013.
[7] J. A. P. Lopes, C. L. Moreira, and A. G. Madureira, "Defining control strategies for microgrids islanded operation," *IEEE Transactions on Power Systems*, vol. 21, no. 2, pp. 916–924, 2006.
[8] A. Mohd, E. Ortjohann, D. Morton, and O. Omari, "Review of control techniques for inverters parallel operation," *Electric Power Systems Research*, vol. 80, no. 12, pp. 1477–1487, 2010.
[9] P. Kundur, *Power System Stability and Control*. McGraw-Hill, 1994.
[10] J. Machowski, J. W. Bialek, and J. R. Bumby, *Power System Dynamics*, 2nd ed. Wiley, 2008.
[11] A. J. Wood and B. F. Wollenberg, *Power Generation, Operation, and Control*, 2nd ed. Wiley, 1996.
[12] M. Andreasson, D. V. Dimarogonas, K. H. Johansson, and H. Sandberg, "Distributed vs. centralized power systems frequency control under unknown load changes," in *European Control Conference*, Zürich, Switzerland, Jul. 2013, pp. 3524–3529.
[13] C. Zhao, U. Topcu, N. Li, and S. Low, "Power system dynamics as primal-dual algorithm for optimal load control," *arXiv preprint arXiv:1305.0585*, 2013.
[14] N. Li, L. Chen, C. Zhao, and S. H. Low, "Connecting automatic generation control and economic dispatch from an optimization view," in *American Control Conference*, 2014, submitted.
[15] E. Mallada and S. H. Low, "Distributed frequency-preserving optimal load control," in *IFAC World Congress*, 2014, submitted.
[16] J. W. Simpson-Porco, F. Dörfler, and F. Bullo, "Synchronization and power sharing for droop-controlled inverters in islanded microgrids," *Automatica*, vol. 49, no. 9, pp. 2603–2611, 2013.
[17] ——, "Voltage stabilization in microgrids via quadratic droop control," in *IEEE Conf. on Decision and Control*, Florence, Italy, Dec. 2013, pp. 7582–7589.
[18] Z. Wang, M. Xia, and M. D. Lemmon, "Voltage stability of weak power distribution networks with inverter connected sources," in *American Control Conference*, Washington DC, USA, Jun. 2013, pp. 6592–6597.
[19] V. Mariani and F. Vasca, "Stability analysis of droop controller inverters via dynamic phasors and contraction theory," in *European Control Conference*, Zürich, Switzerland, Jul. 2013, pp. 1505–1510.
[20] N. Ainsworth and S. Grijalva, "A structure-preserving model and sufficient condition for frequency synchronization of lossless droop inverter-based AC networks," *IEEE Transactions on Power Systems*, vol. 28, no. 4, pp. 4310–4319, 2013.
[21] L.-Y. Lu, "Consensus-based $P-f$ and $Q-\dot{V}$ droop control for multiple parallel-connected inverters in lossy networks," in *IEEE International Symposium on Industrial Electronics*, Taipei, Taiwan, May 2013.
[22] J. Schiffer, R. Ortega, A. Astolfi, J. Raisch, and T. Sezi, "Conditions for stability of droop-controlled inverter-based microgrids," *Automatica*, 2013, submitted.
[23] J. Schiffer, D. Goldin, J. Raisch, and T. Sezi, "Synchronization of droop-controlled autonomous microgrids with distributed rotational and electronic generation," in *IEEE Conf. on Decision and Control*, Florence, Italy, Dec. 2013, pp. 2334–2339.
[24] Q. Shafiee, J. Guerrero, and J. M. Vasquez, "Distributed secondary control for islanded microgrids - a novel approach," *IEEE Transactions on Power Electronics*, 2013, to appear.
[25] H. Liang, B. J. Choi, W. Zhuang, and X. Shen, "Stability enhancement of decentralized inverter control through wireless communications in microgrids," *IEEE Transactions on Smart Grid*, vol. 4, no. 1, pp. 321–331, 2013.
[26] N. Ainsworth and S. Grijalva, "Design and quasi-equilibrium analysis of a distributed frequency-restoration controller for inverter-based microgrids," in *North American Power Symposium*, Manhattan, KS, USA, Sep. 2013.
[27] S. T. Cady, A. D. Domínguez-García, and C. N. Hadjicostis, "A distributed generation control architecture for small-footprint power systems," 2013, submitted.
[28] J. Schiffer, A. Anta, T. D. Trung, J. Raisch, and T. Sezi, "On power sharing and stability in autonomous inverter-based microgrids," in *IEEE Conf. on Decision and Control*, Maui, HI, USA, Dec. 2012, pp. 1105–1110.
[29] J. W. Simpson-Porco, F. Dörfler, Q. Shafiee, J. M. Guerrero, and F. Bullo, "Stability, power sharing, & distributed secondary control in droop-controlled microgrids," in *IEEE Int. Conf. on Smart Grid Communications*, Vancouver, BC, Canada, Oct. 2013, pp. 672–677.
[30] F. Dörfler, M. Chertkov, and F. Bullo, "Synchronization in complex oscillator networks and smart grids," *Proceedings of the National Academy of Sciences*, vol. 110, no. 6, pp. 2005–2010, 2013.
[31] F. Dörfler and F. Bullo, "Novel insights into lossless AC and DC power flow," in *IEEE Power & Energy Society General Meeting*, Vancouver, BC, Canada, Jul. 2013.
[32] J. M. Guerrero, L. GarciadeVicuna, J. Matas, M. Castilla, and J. Miret, "Output impedance design of parallel-connected UPS inverters with wireless load-sharing control," *IEEE Transactions on Industrial Electronics*, vol. 52, no. 4, pp. 1126–1135, 2005.
[33] Y.-H. Moon, B.-H. Cho, T.-H. Rho, and B.-K. Choi, "The development of equivalent system technique for deriving an energy function reflecting transfer conductances," *IEEE Transactions on Power Systems*, vol. 14, no. 4, pp. 1335–1341, 1999.
[34] F. Dörfler and F. Bullo, "On the critical coupling for Kuramoto oscillators," *SIAM Journal on Applied Dynamical Systems*, vol. 10, no. 3, pp. 1070–1099, 2011.
[35] ——, "Kron reduction of graphs with applications to electrical networks," *IEEE Transactions on Circuits and Systems I: Regular Papers*, vol. 60, no. 1, pp. 150–163, 2013.
[36] M. Bürger, D. Zelazo, and F. Allgöwer, "Duality and network theory in passivity-based cooperative control," *arXiv preprint arXiv:1301.3676*, 2013.
[37] S. Boyd and L. Vandenberghe, *Convex Optimization*. Cambridge University Press, 2004.